Polynomial Initial Guess Algorithm for Trajectory Solvers / Optimizers

Ralph Ewig[*]

University of Washington, Seattle, WA, 98195

Most trajectory optimizers have a finite radius of convergence, and the achieved accuracy and required computation time for the converged solution is dependent on the quality of the initial guess. The ideal initial guess algorithm can produce non-optimal, but feasible trajectories in an automated fashion with minimal human oversight. This paper describes a methodology developed to produce initial guess trajectories for a specific (two dimensional) equation of motion set. While the presented example is specific, the described approach is adaptable to any Equations of Motion set of interest. In the presented example, each trajectory solution requires the time history of two control inputs: thrust magnitude and thrust direction. A polynomial based approach in is developed to obtain the desired trajectory, computed in up to three phases (escape, transfer, capture). The trajectories produced by the described algorithm can be roughly categorized into two classes – "fast" trajectories with near straight line geometries, and "slow" trajectories with classical spiral geometries. This paper summarizes the data for typical trajectories in both classes. The developed algorithm is computationally inexpensive and was successfully used in the fully automated derivation of several million trajectories without human intervention.

Nomenclature

A	=	arbitrary constant
α	=	thrust angle
B	=	arbitrary constant
$\hat{e}_r$	=	radial direction unit vector
$\hat{e}_\theta$	=	tangential direction unit vector
EOM	=	Equations Of Motion
$\vec{F}$	=	Force
G	=	Universal gravitational constant
g_0	=	Earth standard gravitational acceleration
μ	=	Gravitational constant of the Sun
I_{SP}	=	Specific impulse
m	=	mass
$\vec{P}$	=	Linear Momentum
$\vec{r}$	=	position vector
R	=	radial distance
SOI	=	Sphere Of Influence
s	=	tangential (angular) position
θ	=	angular coordinate
T	=	Thrust
TOF	=	Time Of Flight
t	=	Time
T/W	=	Thrust to weight ratio
u	=	radial velocity
u_e	=	exhaust velocity
v	=	spacecraft velocity

I. Introduction

The trajectory analysis and optimization work presented in this paper is part of the authors doctoral dissertation research titled "Identification of a Physically-Idealized Human-Rated Rocket-Based Interplanetary Transportation System (PHRITS)"[1]. This work investigated the concept of rocket-based propulsion in fundamental terms, and applies the methodology of Physical Idealization to extrapolate from basic principles the design of the most capable interplanetary transportation system possible within today's understanding of physics. The studies

[*] ralph@open-aerospace.org

implementation required the evaluation of thousands of spacecraft concepts over dozens of mission scenarios. Each mission scenario in turn was evaluated for many possible combinations of departure and destination planets in the solar system, requiring optimized trajectories to be computed for the specific concept, mission scenario, and locations under consideration. Since the process was implemented in a distributed computing environment to be at all feasible[2], the author identified a need for a robust algorithm to generate initial guess trajectories for the optimization process.

Most trajectory optimizers have a limited radius of convergence, and the achieved accuracy and required computation time for the converged solution is dependent on the quality of the initial guess. The ideal initial guess algorithm can produce non-optimal, but feasible trajectories in an automated fashion with minimal human oversight. This paper describes a methodology developed to produce initial guess trajectories for the specific (two dimensional) equation of motion set utilized in the aforementioned research. While the presented example is specific, the described approach is adaptable to any Equations of Motion set of interest. For completeness, the derivation of the EOM set is included in this publication.

In the presented example, each trajectory solution requires the time history of two control inputs: thrust magnitude and thrust direction. A polynomial based approach is developed to obtain the desired trajectory, computed in up to three phases (escape, transfer, capture).

II. Dynamics Model Derivation

In the example application discussed in this paper, the number of concepts and trajectories to be investigated necessitated that the computational demands of the problem be kept at a minimum. Therefore, the dynamics are modeled with a number of simplifying assumptions. It is assumed that all of the trajectory movement is in the plane of the ecliptic and thus two-dimensional only. All planetary orbits are also assumed to be circular and within the ecliptic plane of the solar system.

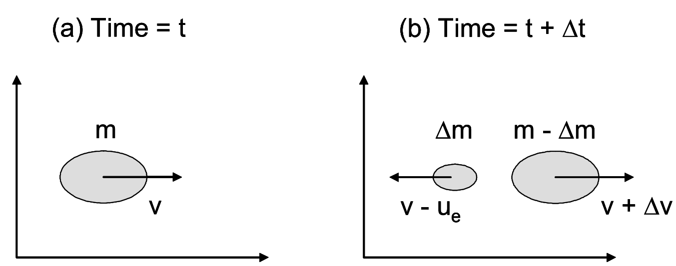

Figure 1. Momentum balance for a rocket spacecraft at (a) initial time, and (b) after expulsion of the exhaust.

A. Coordinate System

With these assumptions, the resulting dynamic model of the spacecraft trajectory is simplified to the movement of a single body under the influence of two forces: (1) a propulsive force (F_P), and (2) the gravitational force of the central body (F_G). The obvious choice of coordinate frame for the problem is non-rotating, polar coordinates. The position vector $\vec{r}$ and its derivatives in polar coordinates are as follows:

$$\vec{r} = R \cdot \hat{e}_r \tag{1}$$

$$\frac{d}{dt}\left(\hat{e}_r\right) = \dot{\theta}\hat{e}_\theta \quad , \quad \frac{d}{dt}\left(\hat{e}_\theta\right) = -\dot{\theta}\hat{e}_r \tag{2}$$

$$\vec{v} = \tfrac{d}{dt}\left(\vec{r}\right) = \dot{R} \cdot \hat{e}_r + R \cdot \tfrac{d}{dt}\left(\hat{e}_r\right) = \dot{R} \cdot \hat{e}_r + R\dot{\theta} \cdot \hat{e}_\theta \tag{3}$$

$$\tfrac{d}{dt}\left(\vec{v}\right) = \left(\ddot{R} - R\dot{\theta}^2\right) \cdot \hat{e}_r + \left(R\ddot{\theta} + 2\dot{R}\dot{\theta}\right) \cdot \hat{e}_\theta \tag{4}$$

B. Equations Of Motion

The Equations of Motion (EOM) are derived from a momentum balance for the complete system of the rocket and its exhaust. The following derivation is a simplified sub-case of the more general derivation developed in Meirovitch.[3] It is important to notice that the force resulting from the rockets thrust is not external to the system and does not initially appear on the left-hand-side of Newton's Law. Consider the finite difference formulation of the system's momentum balance (including any external forces) as illustrated in Figure 1.

At the initial time (left pane), the rocket with mass m is moving at velocity v. At the next moment time (right pane), the exhaust particle Δm is moving away from the rocket at the relative velocity u_e, while the rocket (now with mass reduced by Δm) is moving in the opposing direction at velocity v+Δv.

$$\sum \vec{F}_{ext} = \frac{\Delta \vec{P}}{\Delta t} = \frac{\overline{P}(t+\Delta t) - \overline{P}(t)}{\Delta t} \tag{5}$$

$$\sum \vec{F}_{ext} = \frac{\left[(m - \Delta m)\cdot(\vec{v} + \Delta \vec{v}) + (\vec{v} - \vec{u}_e)\cdot \Delta m\right] - m\vec{v}}{\Delta t} \tag{6}$$

$$\sum \vec{F}_{ext} = m\frac{\Delta \vec{v}}{\Delta t} - (\overline{u}_e + \Delta \vec{v})\frac{\Delta m}{\Delta t} \tag{7}$$

In the limit of Δt and Δv going towards zero this yields the following expression:

$$\sum \vec{F}_{ext} = m \cdot \tfrac{d}{dt}\vec{v} - \tfrac{d}{dt} m \cdot \vec{u}_e \tag{8}$$

Recognizing the term for the thrust of a rocket ($T = \dot{m} \cdot u_e$), and adopting the convention that positive thrust points in the negative velocity direction, the final force / momentum balance is:

$$\sum F_{ext} + T = m \cdot \tfrac{d}{dt}\overline{v} \tag{9}$$

It is now possible to replace the general velocity term with the previously derived expression for the time derivative of velocity in a polar coordinate system. This yields the EOM components in the radial and tangential directions:

$$\sum F_{ext} + T = m \cdot \left[(\ddot{R} - R\dot{\theta}^2)\cdot \hat{e}_r + (R\ddot{\theta} + 2\dot{R}\dot{\theta})\cdot \hat{e}_\theta\right] \tag{10}$$

$$\begin{aligned} \ddot{R} &= \frac{1}{m}\left(\sum F_{ext} + T\right)_r + R\dot{\theta}^2 \\ \ddot{\theta} &= \frac{1}{mR}\left(\sum F_{ext} + T\right)_\theta - \frac{2\dot{R}\dot{\theta}}{R} \end{aligned} \tag{11}$$

In order to obtain the desired information in a form compatible with the intended solution method, the EOM set needs to be expressed as a set of coupled, non-linear, first order differential equations. To that end, the following substitutions are defined:

$$\begin{aligned} &\text{radial position:} && R = r \\ &\text{radial velocity:} && \dot{R} = u \\ &\text{tangential position:} && \theta = s \\ &\text{tangential velocity:} && \dot{\theta} = \frac{v}{r} \end{aligned} \tag{12}$$

Using these definitions and substituting gravity as the only external force component in addition to thrust, the EOM are expressed as follows:

$$
\begin{aligned}
\dot{r} &= u \\
\dot{s} &= \frac{v}{r} \\
\dot{u} &= \frac{1}{m}\left(F_G + T\right)_r + \frac{v^2}{r} \\
\dot{v} &= \frac{1}{m}\left(F_G + T\right)_\theta - \frac{vu}{r}
\end{aligned}
\tag{13}
$$

The gravitational force F_G has by definition only a radial component, with its magnitude derived from the Newton's Law of Universal Gravitation. Similarly, the thrust force can be expressed in terms of its magnitude and direction. It is convenient to decompose it into tangential and radial contributions (Figure 2)

$$
\vec{F}_G = F \cdot \hat{e}_r = -\frac{G \cdot m_1 \cdot m_2}{R^2} \cdot \hat{e}_r = -\frac{\mu m}{R^2} \cdot \hat{e}_r \tag{14}
$$

$$
\vec{F}_P = F_r \cdot \hat{e}_r + F_\theta \cdot \hat{e}_\theta = F_P \sin(\alpha) \cdot \hat{e}_r + F_P \cos(\alpha) \cdot \hat{e}_\theta \tag{15}
$$

$$
\begin{aligned}
F_r &= T/_W \cdot m \cdot g_0 \cdot \sin\alpha - \frac{\mu m}{r^2} \\
F_\theta &= T/_W \cdot m \cdot g_0 \cdot \cos\alpha
\end{aligned}
\tag{16}
$$

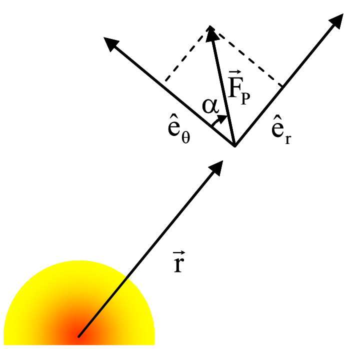

Figure 2. Spacecraft thrust vector coordinate system definition.

The magnitude of the propulsive force F_P was replaced above with the vehicle thrust to weight ratio given by $F_P = T/_W \cdot m \cdot g_0$. Note that the coordinate system as shown in Figure 2 implies that $\hat{e}_\theta$ is the first (i) axis, and $\hat{e}_r$ the second (j) axis, resulting in a definition of α consistent with the right hand rule. Consequently, all trajectories shown in the following discussion are counter-clockwise positive. The last missing component is an expression describing the mass-change of the spacecraft. For the given example a simple relation of $T = \dot{m} \cdot I_{SP} \cdot g_0$ is adopted. The thrust magnitude is normalized by the weight of the spacecraft and replaced with T/W. Together with time itself, the time-dependent quantities in the equation set define the state of the spacecraft at all times. They are referred to as the state-vector (all other quantities of interest can be calculated from them). The thrust angle and magnitude are freely selectable control inputs.

C. Solar System Model

All planetary orbits are assumed to be circular and in the solar ecliptic plane. For planetary destinations, the planet is assumed to be at the desired location when the spacecraft approaches the planet's orbit (achieved by timing the launch appropriately). In most scenarios, the center body will differ during initial escape, transfer, and capture. The problem uses a patched conic approach: the spacecraft is initially in orbit around the departure planet, with the problem formulated in canonical units of the planet. When the spacecraft has left the planets Sphere of Influence (SOI), the problem is transitioned to the Sun as the center body, and heliocentric canonical units. The same approach is used for capture at the destination. All trajectories are positive counter-clockwise in the theta coordinate.

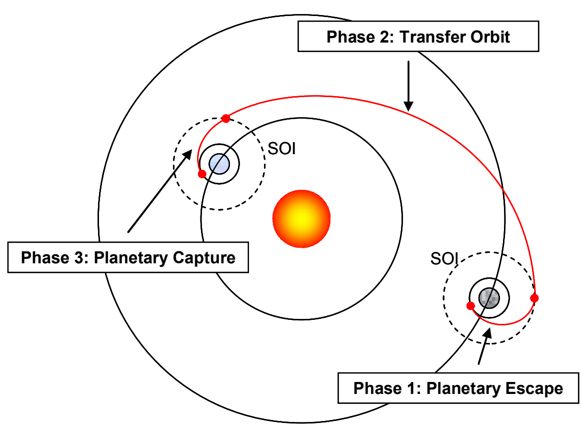

Figure 3. Trajectory phase definition.

III. Initial Guess Algorithm

Most trajectory optimizers have a finite radius of convergence, and the achieved accuracy and required computation time for the converged solution is dependent on the quality of the initial guess. Generally, the most efficient and reliable source is a previously calculated trajectory for the same boundary conditions (departure, destination, TOF), and a concept of a similar configuration. Each trajectory solution requires the time history of the control inputs for thrust magnitude and direction. Time forward integration of the EOM using this control history then results in a desired trajectory that satisfies the imposed constraints (initial / final state, TOF, etc.).

While it is customary for the trained trajectory designer to think of a spacecraft flight path within the context of orbital motions, there is no physical constraint on the trajectory to follow the shape of a Keplerian orbit. As long as a sufficient amount of thrust can be generated, the spacecraft can fly any desired trajectory without violating the EOM – whether that be a traditional Hohmann transfer, a straight line trajectory, or something as unusual as the shape of an octagon. It is therefore possible to pre-suppose a trajectory that satisfies the desired boundary conditions (initial / final position / velocity, TOF, etc.), and then calculate from the EOM the required thrust (control history) to implement it.

A. Trajectory Structure

The trajectories chosen as an initial guess set both the radial position (r) and the tangential velocity (v) to follow the form of a cubic polynomial. The cubic was selected because it provides smooth transitions at the boundaries, and has the correct number of constants to allow for satisfaction of the boundary conditions without requiring the selection of additional (arbitrary) values.

$$\begin{aligned} r(t) &= A_1 t^3 + A_2 t^2 + A_3 t + A_4 \\ v(t) &= B_1 t^3 + B_2 t^2 + B_3 t + B_4 \end{aligned} \tag{17}$$

The constants A and B are determined from the desired boundary conditions of the trajectory: position / velocity at time zero (departure orbit), and at t=TOF (destination orbit).

$$\begin{aligned} r(t=0) &= r_0 & v(t=0) &= v_0 \\ \dot{r}(t=0) &= 0 & \dot{v}(t=0) &= 0 \\ r(t=TOF) &= r_f & v(t=TOF) &= v_f \\ \dot{r}(t=TOF) &= 0 & \dot{v}(t=TOF) &= 0 \end{aligned} \tag{18}$$

This set of boundary conditions defines the constants in the previous expressions, and yields the equations for both parameters:

$$\begin{aligned} r(t) &= \frac{2(r_0 - r_f)}{TOF^3} t^3 - \frac{3(r_0 - r_f)}{TOF^2} t^2 + r_0 \\ v(t) &= \frac{2(v_0 - v_f)}{TOF^3} t^3 - \frac{3(v_0 - v_f)}{TOF^2} t^2 + v_0 \end{aligned} \tag{19}$$

From this equation set all remaining elements of the state vector can be derived. The value for angular position is determined by integration of the tangential velocity, assuming the initial tangential position is zero.

$$s(t) = \int_0^t \frac{v(t)}{r(t)} dt \tag{20}$$

$$u(t) = \frac{6(r_0 - r_f)}{TOF^3} t^2 - \frac{6(r_0 - r_f)}{TOF^2} t \tag{21}$$

Given the values for the derivatives of u and v (from the polynomials above), the values for mass-flow and the control inputs (T, alpha) form a well defined, coupled equation set that can be solved at each time step.

$$\begin{aligned} \dot{u} &= \frac{v^2}{r} + T/_W \cdot g_0 \cdot \sin\alpha - \frac{\mu}{r^2} \\ \dot{v} &= -\frac{v \cdot u}{r} + T/_W \cdot g_0 \cdot \cos\alpha \\ \dot{m} &= \frac{m \cdot T/_W}{I_{SP}} \end{aligned} \tag{22}$$

The first two equations can be rewritten for simplification as follows:

$$\begin{aligned} \underbrace{\frac{1}{g_0}\left(\dot{u} + \frac{v^2}{r} + \frac{\mu}{r^2}\right)}_{A} &= T/_W \cdot \sin\alpha \\ \underbrace{\frac{1}{g_0}\left(\dot{v} + \frac{v \cdot u}{r}\right)}_{B} &= T/_W \cdot \cos\alpha \end{aligned} \tag{23}$$

With this short hand notation, the solution for the thrust magnitude is given by:

$$T/_W = \sqrt{A^2 + B^2} \tag{24}$$

Since the thrust magnitude is required to be positive, the positive of the two roots is selected. The values for mass flow and thrust angle are obtained from the original equation of motion set. The value for specific impulse is selected either as a fixed configuration parameter, or if variable specific impulse is within the concept's capabilities it can be selected in each time step to as closely as possible approximate the theoretical ideal. In this case the resulting exhaust velocity equals the total velocity of the spacecraft (within the bounds of the given concept's specifications).

B. Section Integration

The complete trajectory is calculated in up to three phases (escape, transfer, capture). However, since the initial mass of the spacecraft is not known, but the desired final mass is, the segments are calculated in time reversed order, and integration of the above equation set also is performed in the negative time direction. An initial guess for the TOF of each segment is determined by splitting the total TOF in proportions that will approximate the lowest peak acceleration (thrust requirement) value across the complete scenario. The total TOF is roughly proportional to the square root of the average T/W. and the desired TOF for a given segment can be estimated based on the following expression (where ΔR is the difference in radial distance to be traversed during the segment):

$$TOF_i = TOF \cdot \sqrt{\frac{\Delta R_i}{\sum \Delta R_i}} \tag{25}$$

The segment path-points are set at the boundary of the Sphere Of Influence (SOI) at the departure and destination planets. Based on whether the scenario calls for an inbound or outbound trajectory, the spacecraft is set to leave any given SOI at the closest or farthest away from the Sun. Table 1 summarizes the boundary values imposed for the various segments of a fully integrated three-phase trajectory.

Table 1: Boundary values for initial guess generation.

	Escape	Transfer	Capture
Time	$TOF \cdot \sqrt{\Delta R_{escape} / \sum \Delta R_i}$	$TOF \cdot \sqrt{\Delta R_{transfer} / \sum \Delta R_i}$	$TOF \cdot \sqrt{\Delta R_{capture} / \sum \Delta R_i}$
Position	$r_0 = SOR$ $s_0 = 0$ $r_f = SOI$	$r_0 = r_{departure\_planet} \pm SOI_{departure\_planet}$ $s_0 = 0$ $r_f = r_{destination\_planet} \pm SOI_{destination\_planet}$	$r_0 = SOI$ $s_0 = 0$ $r_f = SOR$
Velocity	$u_0 = 0$ $v_0 = v_{circ@SOR}$ $u_f = 0$ $v_f = 0$	$u_0 = 0$ $v_0 = v_{circ@departure\_planet}$ $u_f = 0$ $v_f = v_{circ@destination\_planet}$	$u_0 = 0$ $v_0 = 0$ $u_f = 0$ $v_f = v_{circ@SOR}$
Mass	$m_f = m_{0@transfer}$	$m_f = m_{0@capture}$	$m_{f\_desired}$

IV. Case Study Trajectory Data

The trajectories produced by the described algorithm can be roughly categorized into two classes – "fast" trajectories with near straight line geometries, and "slow" trajectories with classical spiral geometries. The following sections summarize the data for typical trajectories in both classes. The developed algorithm proved highly reliable in producing trajectories in both categories, with the total number of generated exceeding 5 million. The following data shows the escape, transfer, and capture segments for three Earth / Mars trajectories. The total TOF for the three cases are roughly 450 days, 120 days, and 5 days.

A. Earth Escape

The Earth escape trajectories shown here (Figure 4) start at a circular orbit with an altitude of 383 km, and terminate at the edge of Earth's Sphere Of Influence at 259,000 km. The SOI radius was selected based on the distance where the force on the spacecraft exerted by Earth is roughly equal to the force exerted by the Sun. The distance units in the plot are normalized with the value of the Earth mean equatorial radius.

The TOF for the segments are approximately 6 hours, 6 days, and 23 days. TOF values were selected by subdivision of the TOF for the complete trajectory (escape, transfer, capture) into proportions that achieve roughly identical peak acceleration requirements. The value of the relative radial distance difference of the start and end point in each segment was used as a roughly proportional guideline to determine the segment TOF values.

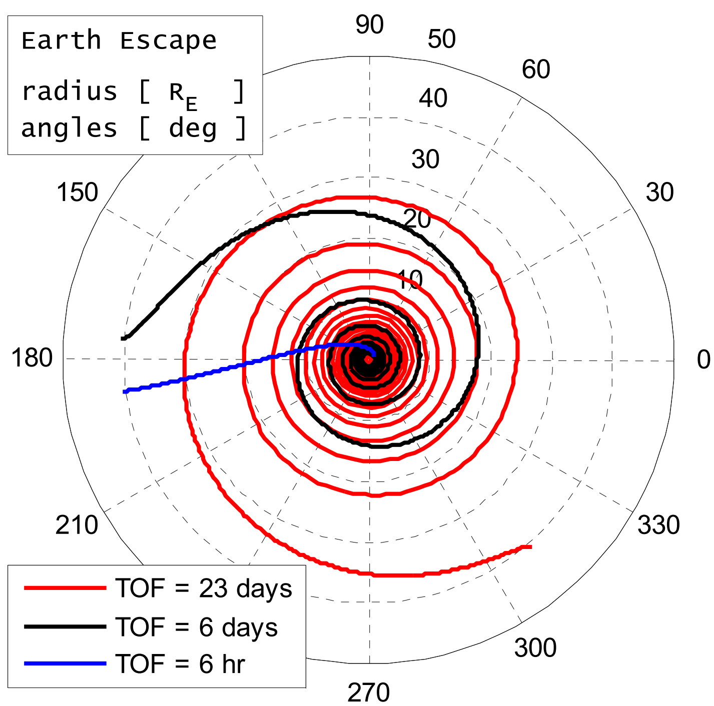

Figure 4. Earth Escape Trajectory.

B. Earth Mars Transfer

Figure 5 shows the Earth / Mars transfer trajectories for the three TOF scenarios. The segment TOF values are 5 days, 107 days, and 410 days. The trajectory starts at the Earth's orbit around the sun (! AU) and terminates at Mars's orbit around the Sun (1.524 AU).

The units shown in the figure are canonical heliocentric. In this simplified solar system dynamics model, it is assumed that the departure window was timed correctly to ensure that the destination planet is at the necessary true anomaly in its orbit when the spacecraft arrives.

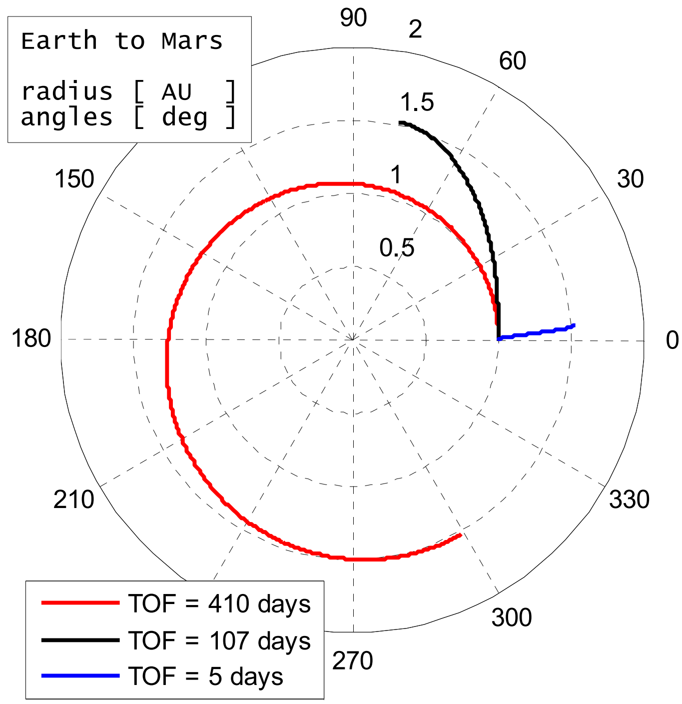

Figure 5. Earth / Mars Transfer Trajectory.

C. Mars Capture

The final segment of the trajectory (capture at Mars) is shown in Figure 6. In this case the segment TOF values for the three scenarios are 4 hours, 4 days and 16 days. The trajectory originates at the edge of Mars' Sphere Of Influence (SOI) determined to have a radius of 129,490 km. The trajectory terminates in a circular orbit around Mars with an altitude of 204 km.

The orbit altitudes for the various destination or departure planets in the PHRITS study were selected with a standard ratio of 1.06 times the mean equatorial radius of the center-body being orbited for all rocky celestial bodies. For gas giants a ratio of 10 was used instead. These values result in standard orbit altitudes that are typical for historical applications (Moon landings, International Space Station, etc.) for solid bodies, and gas giant orbits that are roughly within the "neighborhood" of major moons.

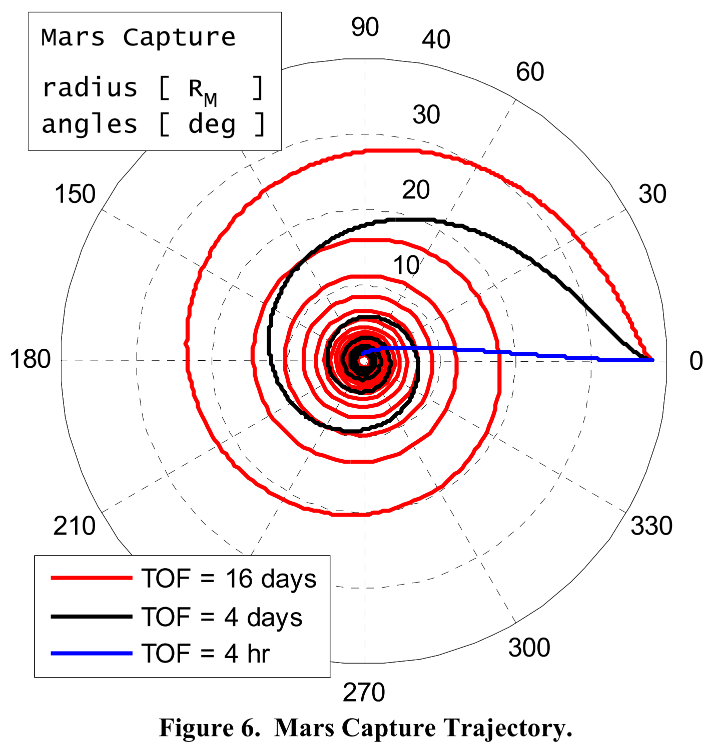

Figure 6. Mars Capture Trajectory.

D. Control History

Figure 7 (next page) shows the control history for all three segments of all three scenarios. Segments are sorted in columns (escape, transfer, capture), and each scenario occupies one row of plots. The time axis shows the total mission TOF across all three segments Control inputs are shown for thrust direction (angle), and thrust magnitude (thrust to weight ratio).

It is interesting to note how not only the peak value for the T/W ratio (thrust magnitude) changes, but also the shape of the curve itself., in spite of the fact that all curves were produced by the same – relatively simple – algorithm. However, all trajectories are continuous thrust, with the thrust direction changing roughly ad midpoint.

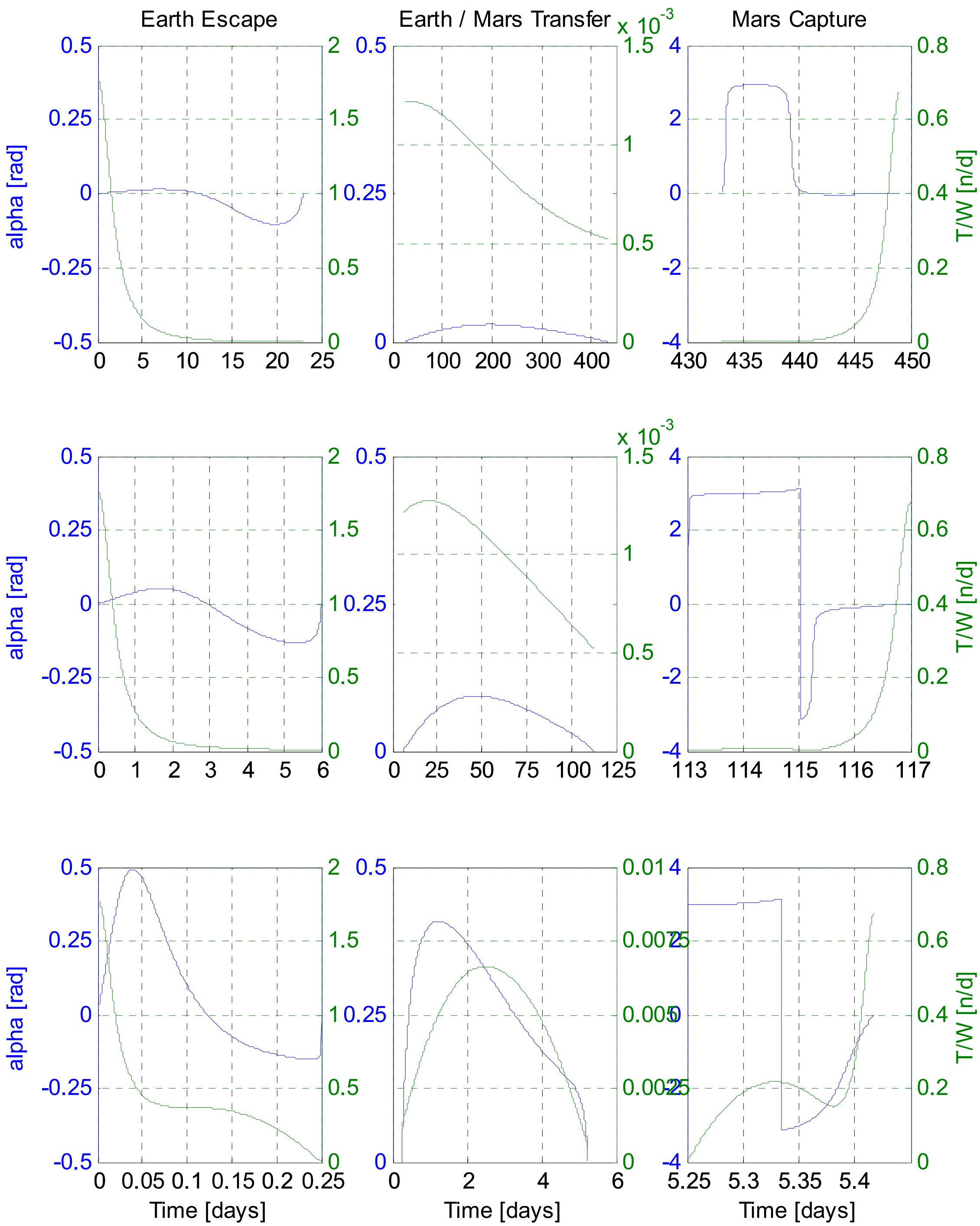

Figure 7. Control History for Escape / Transfer / Capture of all three TOF trajectories..

V. Conclusion

This paper describes an initial guess algorithm for the generation of a wide variety of trajectories in a highly automated fashion. A polynomial based approach is used, based on the concept that a spacecraft can fly any trajectory shape desired as long as sufficient thrust is available. The polynomial algorithm is used to generate a specific trajectory geometry based on desired TOF, initial and final conditions. Subsequently, the control history required to fly the generated trajectory geometry is also calculated. The specific example presented here is for a simplified two-dimensional Equation Of Motion set, applied to the problem of interplanetary transfer orbits within the Solar system. However, the approach taken can easily be extended to any EOM of interest.

Example output data is shown for three scenarios with total TOF values ranging from 5 days to 450 days. The scenario is computed in three trajectory segments (Escape, Transfer, and Capture). The resulting data exhibits an interesting breath of numerical value and characteristic shape, while by definition producing feasible yet sub-optimal solutions well-suited as initial guess trajectories for a numerical optimizer. The data produced by this algorithm should be especially useful in applications where a very large number of trajectories are to investigated in an automated fashion, placing a premium on robustness and minimal user intervention.

References

[1] Ewig, R., "Identification of a Physically-Idealized Human-Rated Rocket-Based Interplanetary Transportation System (PHRITS)", Ph.D. Dissertation, Aeronautics and Astronautics Dept., University of Washington, Seattle, WA 2006

[2] Ewig, R., "Low-Cost Distributed Computing Framework for Large Option Space Trade Studies", Conference on Systems Engineering Research (CSER), International Council On Systems Engineering, paper no. 150, Los Angeles, April 2006.

[3] Meirovitch, Leonard, *Methods of Analytical Mechanics*, McGraw Hill, New York, 2003, pp. 482